THE SINUOSITY OF LUNAR RILLES IN THE ARISTARCHUS PLATEAU. L.J. Chen[1,2], J.E. Bleacher[2], P.D. Lowman[2], [1]Hammond High School, 8800 Guilford Rd., Columbia, MD, 21046, lchen@puuoo.gsfc.nasa.gov, [2]Planetary Geodynamics Laboratory, Code 698, NASA Goddard Space Flight Center, Greenbelt, MD 20771, Jacob.Bleacher-1@nasa.gov, Paul.D.Lowman@nasa.gov.

Introduction: The Aristarchus Plateau is located to the northwest of the lunar nearside (~23.7N/47.4W) covering a surface area of approximately 37,500 km^2. This area is long recognized as a positive topographic feature composed of a complex mix of volcanic and impact related deposits [1-4]. Volcanic features in the Aristarchus Plateau include a variety of vent morphologies, mare lava flows, and the largest and most dense concentration of rilles on the Moon [1].

Lunar rilles are channels that often originate from irregular depressions at their topographic high. They are frequently located axial to slight topographic rises. While it is now generally agreed that rilles are the result of lava flow emplacement, some debate remains as to whether or not they formed through predominantly constructional [5-7] or erosional (either thermal or mechanical) processes [8-11].

Although rilles share many common characteristics, their basic parameters vary greatly, ranging from several kilometers in length and tens of meters in width and depth to 100s of kilometers in length, over a kilometer in width, and 100s of meters in depth [12]. Some rilles decrease in length and width with increased distance from the source vent while others show no change in width. Sinuosity is another parameter that was used to quantitatively catalog some rilles as sinuous, arcuate, or linear [13], and it was suggested that a complete catalog of lunar rille sinuosity might provide insight into the formation of different rille classes [14]. Building on these studies our objective was to quantify the sinuosity of rilles in the Aristarchus Plateau region with the intent of comparing these data to other regions on the Moon.

Approach: Sinuosity has long been a key parameter used in terrestrial river channel classification and analysis, and is easily calculated from remotely sensed images [15,16], making it a reasonable parameter to use for rille characterization [14]. Sinuosity is the ratio of the channel length divided by the straight-line length connecting the origin and the terminus of a feature (Figure 1). Using the Canvas X software we measured rille lengths and straight line lengths, as well as perimeter and area for all identifiable rilles within our study area (16-32N and 40-60W). Our measurements were made on the Clementine 750 nm mosaic (~100 m/pixel), which served as our base map. Additional measurements were made using Apollo 15 and 17 metric images (~40-60m/pix after scanning) and Lunar Orbiter IV frames when available. We plotted rille sinuosity against our measured parameters.

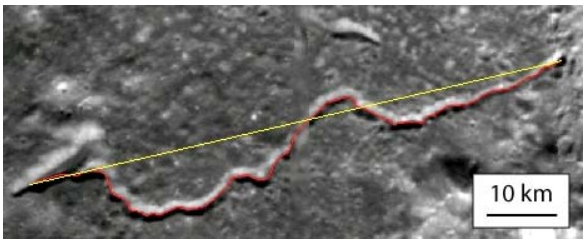

Figure 1. A portion of the Clementine 750 nm global mosaic showing a rille and highlighting the parameters used to calculate sinuosity. The rille's length is outlined in red and its straight line length is outlined in yellow.

Results: We used available Lunar Orbiter images to help identify and measure rilles in the Clementine data, yielding 31 measurements. Sinuosity values ranged between 1.0 and 1.7 for this population of rilles, with only 2 rilles (6%) displaying a sinuosity > 1.5. Analysis of available higher resolution Apollo images, which do not entirely cover the study area, showed that some rilles as mapped in the Clementine data might be composed of more than one feature. As a result, we identified 13-21 additional rilles in the Apollo images that were unnoticed by us in the Clementine images resulting in a complete population of rilles from both data sets between 37 and 52. Sinuosity values for a given rille measured from both Clementine and Apollo images yielded higher values in the Apollo data. The average difference between the two data sets was 0.1.

Using insight gained from our Apollo image analysis we identified some measurements that were related to multiple smaller rilles or anomalous features from our Clementine-derived sinuosity database. Because Apollo images did not provide a consistent resolution or complete coverage of the study area we used the Clementine measurements to plot sinuosity against length, area, and perimeter. When plotted against area and perimeter, no clear trends were revealed. However, sinuosity increases with increased rille length (Figure 2).

Discussion: A number of factors appear to influence the relationship shown in Figure 2. The bulk of the data points cluster below sinuosity values of 1.3 at lengths < 60 km. This sub-group of the study population does not reflect the trend. While there is evidence that sinuosity increases beyond lengths of

50 km, data points are sparse. Therefore, we are not confident that the relationship shown in Figure 2 is statistically significant.

The resolution of the images used also influenced sinuosity measurements. Rilles that were observed in both Clementine and Apollo images yielded higher sinuosity values in the higher resolution images. One cause of the higher sinuosity values is the ability to detect additional detail in rille meanders, thereby increasing the measured length in higher resolution images. Additionally, some rilles are seen to be longer in Apollo images than we were able to detect in the Clementine images alone, particularly for rilles whose widths decrease towards the terminus.

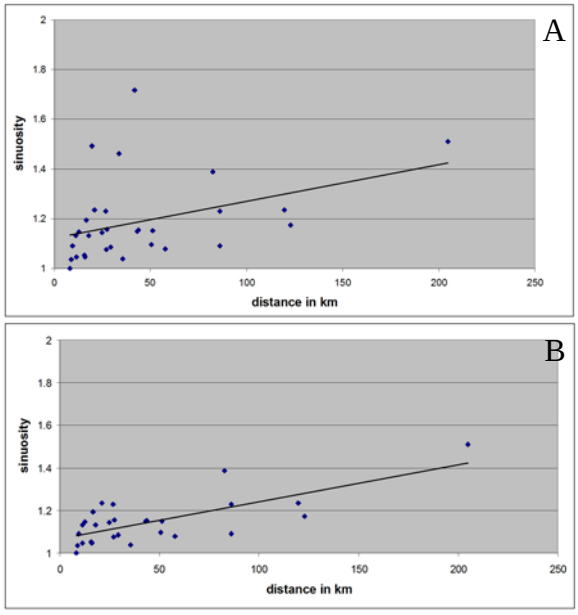

Figure 2. Plots showing rille sinuosity on the y-axis and rille length in kilometers on the x-axis as measured using the Clementine 750 nm global mosaic. Plot A shows all rilles measured in the Clementine data, and Plot B shows the same data with possible anomalous rilles removed. Both plots show a linear trend line suggesting an increase in sinuosity associated with increased rille length.

Another issue when using different resolution images is potential difficulty in defining the extent of a rille. In some cases Apollo images showed that rilles that were mapped in Clementine data might better be classified as two or more rilles. For example, the continuous channel shown in Figure 3 might be considered as one rille. However, there appear to be three different irregular depressions that might represent three sources, and each of these segments displays a different sinuosity. As such, this feature could be considered three rilles, shown in red, blue, and yellow, that are spatially superposed on each other. Another interpretation could be that the red and blue rilles display similar widths while the yellow rille is wider, suggesting that two rilles are present. Additionally, some rilles thought to be two adjacent rilles based on Clementine data analysis were identified as one longer rille for which entire segments of the rille were not visible in the coarser resolution image.

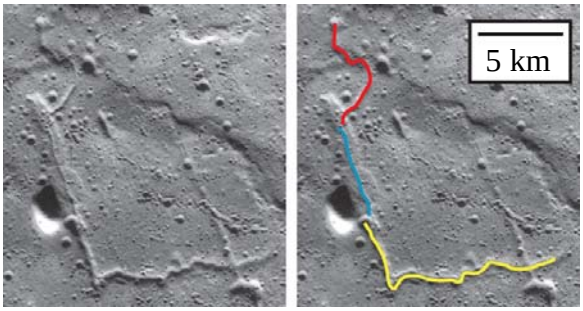

Figure 3. An Apollo 15 image showing a continuous rille that might also be subdivided into two or three rilles (shown in red, blue, and yellow on the left) based on sinuosity, width, and source depressions.

Conclusion and Future Work: The sinuosity of rilles in the Aristarchus region displays a positive correlation with increased rille length as measured with Clementine data. However, comparisons with Apollo images suggest that additional work is needed to clarify this relationship. It was suggested that a complete catalog of lunar rille sinuosity would provide insight into the formation of these features [14]. As such, the results presented here are a preliminary step in developing such a catalog. While the Clementine 750 nm mosaic provides global coverage, our analysis of Apollo data suggests that image resolutions of 10-60 m/pixel would best enable this type of study.

References: [1] Zisk et al. (1977) *Moon*, **17**, 59. [2] Lucey et al. (1986) *JGR*, **91(B4)**, D344. [3] McEwen et al. (1994) *Science*, **266**, 1858. [4] Le Mouelic et al. (2000) *JGR*, **105(E4)**, 9445. [5] Oberbeck et al. (1969) *Modern Geology*, **1**, 75. [6] Greeley (1971) *Science*, **172**, 722. [7] Gornitz (1973) *The Moon*, **6**, 337. [8] Hulme (1973) *Modern Geology*, **4**, 107. [9] Carr (1974) *Icarus*, **22**, 1. [10] Head and Wilson (1981) *LPSC XII*, 427. [11] Honda and Fujimura (2005) *LPSC XXXVI*, #1562. [12] Swann (1988) *LPSC XIX*, 1163. [13] Oberbeck et al. (1971) NASA Tech. Memo., TM X-62,088. [14] Oberbeck et al. (1972) NASA SP-315, 29-80. [15] Leopold and Wolman (1957) USGS Prof. Paper, 282B. [16] Rosgen (1994) *Catena*, **22**, 169.